Proceedings of the
44th IEEE Conference on Decision and Control, and
the European Control Conference 2005
Seville, Spain, December 12-15, 2005

Sliding mode tracking control of output voltage in multiple modular boost power converters using the method of stable system center

Joe Patterson, and Yuri B. Shtessel, *Senior Member, IEEE*

Abstract— **Application of sliding mode control to the direct tracking of an arbitrary output voltage profile in multiple modular DC-to-DC boost power converters is studied. In particular, the case of two boost converters sharing a common primary source of electric supply (PSES) and driving independent loads is studied to demonstrate tracking control of multiple modular converters. Operating point analysis shows that the coupled converters have two possible operating points, which result in nonminimum phase operation. It is demonstrated that one of these operating points results in a practical and physically realizable solution while the other does not. Sliding mode control by the method of stable system center is employed, and the nonminimum phase output tracking problem is reduced to a state-tracking problem. A numerical example and simulation demonstrates the effectiveness of the sliding mode control design.**

I. Introduction

Switched mode DC-to-DC power converters are used in a variety of electric power supply systems, including cars, ships, aircraft and computers [1]. Application of Sliding Mode Control [2,3] in tracking a real-time voltage profile is very promising because a switching control strategy is traditionally employed in power converters, and because of the inherent robustness properties of the sliding mode. A number of contributions to sliding mode control [2,3] of power converters are available in the papers [1,4-12]. Direct regulation/tracking control of the output voltage for multiple modular buck and buck-boost converters has previously been addressed in the paper [5] and so this work is intended to extend this concept to the study of multiple modular boost converters. It has been shown in [4,6,7,9,10] that controlling the current can indirectly control the output voltage in ideal converters. In the papers [11,12], a sliding mode control design technique called the method of stable system center, which allows direct control of the voltage in ideal boost and buck-boost converters is developed. The technique is based on the transformation of nonminimum phase output tracking in causal systems to state variable tracking. The bounded state reference profiles are generated using custom-designed equations of the system center [14].

Primary sources, including chemical batteries, solar cells, and rotating generators, have internal resistance. The contribution of this paper is in the analysis and direct control of the output voltage of multiple modular DC-to-DC boost power converters connected in parallel sharing a common voltage source that includes the source resistance. Source resistance should be considered because of the power limiting and coupling effects. The method of stable system center is employed and results in high fidelity output voltage tracking and decoupling for this nonminimum phase system.

Operating point analyses are conducted, and it is shown in this paper that parallel boost converters sharing a common power source and driving independent loads have two possible operating points for each converter and that the system is nonminimum phase for either operating point. Both operating points are explored and it is shown that one operating point is useful while the other is not due to very large inductor currents.

The paper is organized as follows: Section II is dedicated to the mathematical modeling of parallel boost converters including source resistance. In Section III the stability of the forced zero dynamics and operating point analyses are presented. Section IV presents the method of stable system center in nonminimum phase output tracking. The nonminimum phase output tracking problem solution for parallel boost converters driven by a common source that includes source resistance and driving independent loads is presented in Section V. In Section VI a numerical example and simulation of the parallel boost converter is discussed. Conclusions are summarized in Section VII.

II. Mathematical model of Multiple Modular Boost converters

Analysis and control of multiple modular, and this case specifically, two paralleled DC-to-DC power converters should take source resistance, R_s, of the primary source of electric power supply into account. The parallel boost converters (Fig. 1) can be modeled as bilinear systems. The natural state variables are the current through the inductors and the voltage across the capacitors. The variables of Figure 1 are as follows: v_{ci} are the voltages across the capacitors, i_{Li} are the currents through the inductors, E is the ideal source voltage, R_s is the source resistance, R_{Li} are the load resistances, L_i are the inductances, and C_i are the capacitances. The subscript $i = 1, 2$ hereon.

Joe Patterson is with the U.S. Army Aviation and Missile Command; Research, Development, and Engineering Center, Redstone Arsenal, AL 35808, USA (email: Joe.Patterson@amrdec.army.mil).

Yuri Shtessel is with the Electrical Engineering Department, University of Alabama in Huntsville, Huntsville, AL 35899 USA, (email: Shtessel@ece.uah.edu, tel: (256) 824-6164, fax: (256) 824-6803).

0-7803-9568-9/05/$20.00 ©2005 IEEE

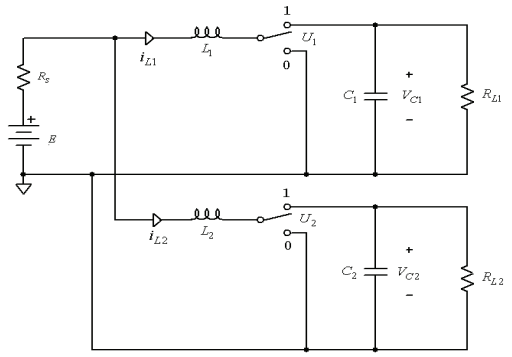

Fig. 1. Parallel (multiple modular) boost converter circuit with source resistance.

The plant is described by the following system of differential equations:

$$\frac{dx_1}{d\tau} = -\alpha x_1 - x_2(1-u_1) - \alpha x_3 + 1 \quad (1a)$$

$$\frac{dx_2}{d\tau} = x_1(1-u_1) - \gamma_1 x_2 \quad (1b)$$

$$\frac{dx_3}{d\tau} = -\alpha x_1 - \alpha x_3 - x_4(1-u_2) + 1 \quad (1c)$$

$$\frac{dx_4}{d\tau} = x_3(1-u_2) - \gamma_2 x_4 \quad (1d)$$

with

$$x_1 = \frac{1}{E}\sqrt{\frac{L_1}{C_1}}i_{L_1}, x_2 = \frac{1}{E}v_{C_1}, x_3 = \frac{1}{E}\sqrt{\frac{L_2}{C_2}}i_{L_2}, x_4 = \frac{1}{E}v_{C_2}, \tau = \frac{t}{\sqrt{L_1 C_1}} \quad (1e)$$

where τ is the scaled time variable, and t denotes real time. $u \in \{0,1\}$ is a switching control function that can be equal to one or zero. To simplify the analysis, the mathematical model will from here forward assume that the power converters are identical, e.g., the converters have the same values of L and of C. As such the source resistance and load resistances are represented in (1) by

$$\alpha = R_s\sqrt{\frac{C}{L}}, \gamma_i = \frac{1}{R_{Li}}\sqrt{\frac{L}{C}}.$$

III. Stability of Forced Zero Dynamics and Operating Point Analysis

Before the output voltage-tracking controller is designed it is necessary to identify if the system (1) is minimum or nonminimum phase. This is defined by the stability analysis of the forced zero dynamics of the system in (1). In order to study stability of the forced zero dynamics, a transformation of the system in (1) is performed to put the system into the normal canonical form [13], having in mind that we are seeking tracking control of the output voltages x_2 and x_4. This eliminates the control variable u_i from equations (1a) and (1c) so that the internal dynamics may be studied. Transformation variables z_i and ξ_i are introduced and results in the equations (2). They are analogous to the inductor currents and the output voltages respectively.

$$\dot{z}_1 = -2\alpha(z_1 - \xi_1) - 2\alpha\sqrt{z_1 - \xi_1}\sqrt{z_2 - \xi_2} + 2\sqrt{z_1 - \xi_1} - 2\gamma_1\xi_1 \quad (2a)$$

$$\dot{z}_2 = -2\alpha(z_2 - \xi_2) - 2\alpha\sqrt{z_1 - \xi_1}\sqrt{z_2 - \xi_2} + 2\sqrt{z_2 - \xi_2} - 2\gamma_2\xi_2 \quad (2b)$$

$$\dot{\xi}_1 = 2\sqrt{\xi_1(z_1 - \xi_1)}\cdot(1-u_1) - 2\gamma_1\xi_1 \quad (2c)$$

$$\dot{\xi}_2 = 2\sqrt{\xi_2(z_2 - \xi_2)}\cdot(1-u_2) - 2\gamma_2\xi_2 \quad (2d)$$

The control function is $v_i \in [-0.5, 0.5]$: $v_i = u_i - 0.5$ and is substituted into (2). The internal variables $z_i = x_1^2 + x_2^2$, $z_2 = x_3^2 + x_4^2$ and the controlled outputs are $\xi_1 = x_2^2$, $\xi_2 = x_4^2$. It is worthwhile mentioning that in the ideal case z is the flat output [16]. Note that in terms of (2), we require the design of switching controls v_i that provides for asymptotic output tracking of an arbitrary real-time and sufficiently smooth command profile $\xi_{c_i}(t)$. We wish to provide

$$\lim_{t\to\infty}\left|\xi_{c_i}(t) - \xi_i(t)\right| = 0. \quad (3)$$

The output tracking problem (3) is equivalent to the tracking of the arbitrary command profile of output voltages, since $\xi_i = x_i^2$. In order to conduct stability analysis of the forced zero dynamics, we linearize the nonlinear equation of the internal dynamics given in (2a), (2b) nearby the operating points (z_{10}, ξ_{10}) and (z_{20}, ξ_{20});

$$\begin{aligned}\dot{z}_1 &= \left(\alpha\frac{\sqrt{z_{20}-\xi_{20}}}{\sqrt{z_{10}-\xi_{10}}} - \frac{1}{\sqrt{z_{10}-\xi_{10}}} + 2\alpha - 2\gamma_1\right)\xi_1 \\ &+ \left(\alpha\frac{\sqrt{z_{10}-\xi_{10}}}{\sqrt{z_{20}-\xi_{20}}}\right)\xi_2 + \left(-\alpha\frac{\sqrt{z_{20}-\xi_{20}}}{\sqrt{z_{10}-\xi_{10}}} + \frac{1}{\sqrt{z_{10}-\xi_{10}}} - 2\alpha\right)z_1 \\ &+ \left(-\alpha\frac{\sqrt{z_{10}-\xi_{10}}}{\sqrt{z_{20}-\xi_{20}}}\right)z_2 + \sqrt{z_{10}-\xi_{10}} \\ \dot{z}_2 &= \left(\alpha\frac{\sqrt{z_{20}-\xi_{20}}}{\sqrt{z_{10}-\xi_{10}}}\right)\xi_1 + \left(\alpha\frac{\sqrt{z_{10}-\xi_{10}}}{\sqrt{z_{20}-\xi_{20}}} - \frac{1}{\sqrt{z_{20}-\xi_{20}}} + 2\alpha - 2\gamma_2\right)\xi_2 \\ &+ \left(-\alpha\frac{\sqrt{z_{20}-\xi_{20}}}{\sqrt{z_{10}-\xi_{10}}}\right)z_1 + \left(-\alpha\frac{\sqrt{z_{10}-\xi_{10}}}{\sqrt{z_{20}-\xi_{20}}} + \frac{1}{\sqrt{z_{20}-\xi_{20}}} - 2\alpha\right)z_2 \\ &+ \sqrt{z_{20}-\xi_{20}}\end{aligned} \quad (4)$$

and replace the output variables ξ_i by the arbitrary real-time command profiles $\xi_{ci}(t)$.

The operating points $[z_{i0}, \xi_{i0}]^T$ are defined as equilibrium points in (4) by setting $\dot{z}_i = 0$.

Letting $q_i = \sqrt{z_{i0} - \xi_{i0}}$ simplifies the stability and operating point analyses. Substitution into (4) and putting the internal dynamics into matrix form yields:

$$Q_1 = \begin{bmatrix} -\alpha\dfrac{q_2}{q_1} + \dfrac{1}{q_1} - 2\alpha & -\alpha\dfrac{q_1}{q_2} \\ -\alpha\dfrac{q_2}{q_1} & -\alpha\dfrac{q_1}{q_2} + \dfrac{1}{q_2} - 2\alpha \end{bmatrix} \tag{5}$$

Conducting eigenanalysis on (5) gives two conditions that must be met for stability (minimum phase condition):

$$\alpha_1 > \frac{1}{(q_1 + q_2) + \left(\dfrac{2q_1q_2}{q_1 + q_2}\right)} \tag{6}$$

$$2(q_1 + q_2)^2\alpha^2 - 3(q_1 + q_2)\alpha + 1 > 0 \tag{7}$$

Obviously, there are two solutions to (7). Solving and simplifying the solutions of (7) yields

$$\alpha_2 = \frac{1}{2(q_1 + q_2)}, \alpha_3 = \frac{1}{q_1 + q_2}. \tag{8}$$

Because both conditions (6), (7) must be met per the eigenanalysis, it is necessary to determine which solutions in (6) or (8) provide for stability. This condition is found by determining which of these solutions meet both stability conditions simultaneously. Some algebraic manipulation of inequalities and the requirements of eigenanalysis determined that the valid stability condition is given by

$$\alpha > \frac{1}{q_1 + q_2}. \tag{9}$$

Now we proceed to the operating point analysis. It is desirable to have the source resistance R_S small, otherwise the power losses, $\left(i_{L1}^2 + i_{L2}^2\right)R_S$ could become large which results in reduced overall efficiency. Since the parameter α is proportional to R_S, it makes sense to study the equilibrium point behavior while $\alpha \to 0$. By setting $\dot{z}_i = 0$ the equilibrium points can be determined. Algebraic manipulation of (4) results in two quadratic equations for the equilibrium points.

$$\alpha q_1^2 + \alpha q_1 q_2 - q_1 + \gamma_1\xi_{10} = 0 \tag{10}$$

$$\alpha q_2^2 + \alpha q_1 q_2 - q_2 + \gamma_2\xi_{20} = 0 \tag{11}$$

Solving (10), (11) simultaneously yields two solution sets

$$q_i = \frac{2\gamma_i\xi_{i0}}{1 - \sqrt{1 - 4\alpha(\gamma_1\xi_{10} + \gamma_2\xi_{20})}}, \forall i = \overline{1,2} \tag{12}$$

and

$$q_i = \frac{2\gamma_i\xi_{i0}}{1 + \sqrt{1 - 4\alpha(\gamma_1\xi_{10} + \gamma_2\xi_{20})}}, \forall i = \overline{1,2} \tag{13}$$

Now it is necessary to determine which equilibrium point, (12) or (13) is useful from a practical standpoint, and whether or not they are minimum or nonminimum phase. This may be determined by taking the limit of the inductor currents at the equilibrium point as $\alpha \to 0$. Since $q_i = \sqrt{z_{i0} - \xi_{i0}}$ then the limits of the current from the equilibrium points (12) are

$$\begin{aligned} \lim_{\alpha\to 0} z_{i0} &= \xi_{i0} + \left(\frac{2\gamma_i\xi_{i0}}{1 - \sqrt{1 - 4\alpha(\gamma_1\xi_{10} + \gamma_2\xi_{20})}}\right)^2 \\ &= \xi_{i0} + \left(\frac{2\gamma_i\xi_{i0}}{0}\right)^2 \to \infty, \forall i = \overline{1,2} \end{aligned} \tag{14}$$

The limits of the current from the equilibrium points (13) are

$$\begin{aligned} \lim_{\alpha\to 0} z_{i0} &= \xi_{i0} + \left(\frac{2\gamma_i\xi_{i0}}{1 + \sqrt{1 - 4\alpha(\gamma_1\xi_{10} + \gamma_2\xi_{20})}}\right)^2 \\ &= \xi_{i0} + \left(\frac{2\gamma_i\xi_{i0}}{2}\right)^2 \to \xi_{i0} + (\gamma_i\xi_{i0})^2, \forall i = \overline{1,2} \end{aligned} \tag{15}$$

Clearly, the inductor current in equilibrium point (12) is not tractable as the source resistance becomes small. Since the inductor current in (13) has a limit, it is the practical equilibrium point to take. It should also be noted that for a real operating point to exist the condition (16) must be met as well.

$$1 - 4\alpha\left(\gamma_1\xi_{10} + \gamma_2\xi_{20}\right) > 0 \tag{16}$$

It is necessary to determine the system type given the chosen equilibrium point in (13). In order for the system to be minimum phase, the stability requirement (9) must be met otherwise the system is nonminimum phase. Rearranging (9),

$$q_1 + q_2 > \frac{1}{\alpha}. \tag{17}$$

Adding q_1, q_2 from (12),(13) gives

$$q_1 + q_2 = \frac{1 - \sqrt{1 - 4\alpha(\gamma_1\xi_{10} + \gamma_2\xi_{20})}}{2\alpha}$$

Applying the inequality of (18),

$$\frac{1 - \sqrt{1 - 4\alpha(\gamma_1\xi_{10} + \gamma_2\xi_{20})}}{2\alpha} > \frac{1}{\alpha} \tag{18}$$

If (18) holds true, it necessarily implies stability and thus minimum phase at the equilibrium point in (13). Otherwise the system is nonminimum phase. To simplify this analysis let

$$\omega = \gamma_1\xi_{10} + \gamma_2\xi_{20}. \tag{19}$$

Substituting (19) into (18) and solving the resulting inequality gives

$$\sqrt{1 - 4\alpha\omega} < -1. \tag{20}$$

It is obvious that (20) can never be true. This implies instability of the forced zero dynamics. As such, the system is nonminimum phase. Because of the nonminimum phase nature of the system, traditional sliding mode control techniques cannot be applied and so a more advanced technique, the method of stable system center shall be employed to solve the control problem. Although not shown, it should be mentioned that the operating point in (12) also results in a nonminimum phase system as well.

In this paper we design an output voltage-tracking controller for parallel causal boost converters that include a source resistance in (2) nearby the second operating point (13). This is a nonminimum phase output-tracking problem. A similar problem for a single ideal causal boost converter

was addressed in [11,12] using the method of stable system center [14]. In this paper we also use this method [14] to address the output-tracking problem in the parallel boost converters with source resistance.

The problem at hand is to design the control v_i that forces the output variable ξ_i to asymptotically track the command profile $\xi_{ci}(t)$ is given by an exogenous system with a known stable characteristic polynomial

$$P_k(\lambda) = \lambda^k + p_{k-1}\lambda^{k-1} + \cdots + p_1\lambda + p_0 \quad (21)$$

where k is the order of the exogenous system, and $p_{k-1}, \cdots, p_1, p_0$ are specified non-negative constants.

IV. The Method of Stable System Center in Nonminimum Phase Output Tracking

The results [14] are formulated for the following non-minimum phase system:

$$\begin{cases} \dot{\psi} = Q_1\psi + Q_2 y + f(t) \\ \dot{y} = \varphi(y,\psi,t) + \omega(y,\psi)u \end{cases} \quad (22)$$

where $\psi(t) \in \Re^{n-m}$ is the internal state, $y(t) \in \Re^m$ the controlled vector output, $u(t) \in \Re^m$ the control function; $\varphi(\cdot) \in \Re^m$ is a bounded vector field and $\omega(\cdot) \in \Re^{m\times m}$ is a non-singular matrix; $Q_1 \in \Re^{(n-m)\times(n-m)}$ is a known non-singular non-Hurwitz matrix, $Q_2 \in \Re^{(n-m)\times m}$ is a known matrix, the pair (Q_1, Q_2) is completely controllable; $f(t)$ is an unmatched norm-bounded [2,3] external disturbance.

Remark. System (22) is nonminimum phase, since $Q_1 \in \Re^{(n-m)\times(n-m)}$ is a non-Hurwitz matrix that yields instability of the zero dynamics.

The problem is to provide the asymptotic tracking of a causal smooth command (tracking) profile, $y \to y_c(t)$ as time increases, in the presence of an unmatched external disturbance $f(t)$ that can be measured or estimated using high order sliding mode differentiation/estimation technique [15]. The stable system center $\tilde{\psi}_c(t)$ can be computed using the following theorem.

Theorem 1 [14] Given the nonminimum phase system (15) with the measurable state vector (ψ, y) and the following set of conditions:

1. The matrix $\tilde{Q}_1$ in (22) is non-Hurwitz and nonsingular.
2. The output reference profile $y_c(t)$ and the unmatched disturbance $f(t)$ can be piecewise represented by a known linear exosystem with a characteristic polynomial given by (21).

Then

1. The output tracking in real time of the bounded reference profile, $y_c(t) \in \Re^m$, can be replaced by tracking the state reference profile $(\psi_c, y_c)^T \in \Re^n$, such that $(\psi, y)^T \to (\psi_c, y_c)^T$ asymptotically with given eigenvalues.
2. The internal state reference profile $\tilde{\psi}_c \in \Re^{n-m}$ is generated by the matrix differential equation

$$\begin{aligned} &\tilde{\psi}_c^{(k)} + c_{k-1}\tilde{\psi}_c^{(k-1)} + \cdots + c_1\dot{\tilde{\psi}}_c + c_0\psi_c \\ &\quad = -(P_{k-1}\theta_c^{(k-1)} + \cdots + P_1\dot{\theta}_c + P_0\theta_c), \end{aligned} \quad (23)$$

where the constants $c_{k-1,\ldots,}c_1, c_0$ are chosen to provide any desired eigenvalues for $\tilde{\psi}_c \to \psi_c$, and the matrices $P_{k-1}, \ldots, P_1, P_0 \in \Re^{(n-m)\times(n-m)}$ are given by

$$\begin{aligned} P_{k-1} &= (I + c_{k-1}Q_1^{-1} + \cdots + c_0Q_1^{-k}) \cdot (I + p_{k-1}Q_1^{-1} + \cdots + p_0Q_1^{-k})^{-1} - I \\ P_{k-2} &= c_{k-2}Q_1^{-1} + \cdots + c_0Q_1^{-(k-1)} - (p_{k-1} + I) \cdot (p_{k-2}Q_1^{-1} + \cdots + p_0Q_1^{-(k-1)}) \\ &\cdots \\ P_1 &= c_1Q_1^{-1} + c_0Q_1^{-2} - (p_{k-1} + I) \cdot (p_1Q_1^{-1} + p_0Q_1^{-2)}) \\ P_0 &= c_0Q_1^{-1} - (p_{k-1} + I) \cdot p_0Q_1^{-1)}) \end{aligned} \quad (24)$$

3. The term $\theta_c(y_c, \hat{f}) = Q_2 y_c + \hat{f}$ in (22) is estimated.

Proof. See [14]

Now we can use the stable system center $\tilde{\psi}_c(t)$ for $\psi_c(t)$ when computing the sliding surface keeping in mind that $\tilde{\psi}_c(t) \to \psi_c(t)$ as time increases. Hence, the sliding mode equations will converge asymptotically.

V. Output Voltage Tracking Control for Multiple Modular Boost Converters

To apply the method of stable system center presented in Section IV to the output voltage tracking in the parallel boost converter system, we must represent (2) in the form of (22). To achieve this, the internal dynamics are linearized as in (4) while the nonlinear input-output dynamics are retained. Previously we obtained the linearized internal dynamics, and the system, which is valid near the operating point $[z_{i0}, \xi_{i0}]^T$ in (4).

We assume output-tracking (command) profiles and the term Γ in (4) are described by an exogenous system of linear time-invariant differential equations with the following characteristic equation:

$$P_3(\lambda) = \lambda^3 + 0 \cdot \lambda^2 + \omega_n^2 \cdot \lambda + 0 \quad (25)$$

It means, for instance, that the causal command profiles could be of the form

$$\xi_{ci} = A_i + B_i \sin(\omega_{ni}t + \phi_i) \quad (26)$$

where A_i, B_i and ϕ_i are unknown piecewise constants, ω_{ni} is a known piecewise constant. The term Γ in (4) that falls into (25) is assumed to be piecewise constant.

The operating point in (13) is used. Letting $z_i \to z_{ci}$ and $\xi_i \to \xi_{ci}$ in (4) and substituting (26) gives the equation of system center, which is, in matrix form:

$$\dot{Z}_c = Q_1 Z_c + Q_2 \Xi_c + \Gamma \tag{27}$$

Where Q_1 is given by (5), and Q_2, Γ are given by (28) as follows:

$$Q_2 = \begin{bmatrix} \alpha\frac{q_2}{q_1} - \frac{1}{q_1} + 2\alpha - 2\gamma_1 & \alpha\frac{q_1}{q_2} \\ \alpha\frac{q_2}{q_1} & \alpha\frac{q_1}{q_2} - \frac{1}{q_2} + 2\alpha - 2\gamma_2 \end{bmatrix} \tag{28}$$

$$\Gamma = \begin{bmatrix} q_1 \\ q_2 \end{bmatrix} = \begin{bmatrix} \sqrt{z_{10} - \xi_{10}} \\ \sqrt{z_{20} - \xi_{20}} \end{bmatrix}$$

$$\Xi_c = \begin{bmatrix} \xi_{1c} \\ \xi_{2c} \end{bmatrix} = \begin{bmatrix} A_1 + B_1 \sin(\omega_n t + \phi_1) \\ A_2 + B_2 \sin(\omega_n t + \phi_2) \end{bmatrix}$$

and (27) is unstable as shown in the stability analysis of Section III. Now the equation of the system center can be written in accordance with (23) as

$$\tilde{z}_c^{(3)} + c_2\tilde{z}_c^{(2)} + c_1\tilde{z}_c + c_0\tilde{z}_c = -(P_2\theta_c^{(2)} + P_1\theta_c^{(1)} + P_0\theta_c), \tag{29}$$

where

$$\theta_c = Q_2\Xi_c + \Gamma \tag{30}$$

The characteristic polynomial of the exogenous system that describes the signal θ_c is obtained from (21) and (25) with $p_2 = 0,\ p_1 = \omega_n^2,\ and\ p_0 = 0.$ The coefficients $P_0, P_1, and\ P_2$ are computed in accordance with (24) and where $k = 3$. For this particular case these are given in (31) where Q_1, Q_2 are given in (5), (28) respectively.

$$P_0 = c_0 Q_1^{-1} - (P_2 + I)\cdot\left(p_0 Q_1^{-1}\right)$$

$$P_1 = c_1 Q_1^{-1} + c_0 Q_1^{-2} - (P_2 + I)\cdot\left(p_1 Q_1^{-1} + p_0 Q_1^{-2}\right) \tag{31}$$

$$P_2 = (I + c_2 Q_1^{-1} + c_1 Q_1^{-2} + c_0 Q_1^{-3})\cdot\left(I + p_2 Q_1^{-1} + p_1 Q_1^{-2} + p_0 Q_1^{-3}\right)^{-1} - I$$

The matrices of (31) are generally too complex to solve symbolically for anything other than a simple scalar case, thus, (31) these are computed and used in the numerical example and simulation.

Remark. The stable (bounded) system center $\tilde{z}_c$, defined by (29), (30), and (31), converges asymptotically to a bounded solution of the unstable equation of the system center (27), z_c, i.e., $\tilde{z}_c \to z_c$, as time increases in accordance with Theorem 1. Since the switching control functions v_i can take on values of 0.5 or –0.5, the following sliding mode controller is selected:

$$v = -0.5 \cdot SIGN(\sigma) \tag{32}$$

where $SIGN(\sigma) = \left[sign(\sigma_1), sign(\sigma_2)\right]^T$.

The switching functions are defined as

$$\sigma = e_\xi + K\tilde{e}_z, \quad K \in \Re^{2\times 2},\ e_\xi = \Xi_c - \Xi, \quad \Xi = \left[\xi_1, \xi_2\right]^T \tag{33}$$

Assume that the sliding mode exists on the switching surface $\sigma_i = 0$. Then the matrix K is selected on the basis of the desired tracking error dynamics in the sliding mode, given in vector-matrix form as in (34).

$$\dot{\tilde{e}}_z = (Q_1 - KQ_2)\tilde{e}_z + \left(\dot{\tilde{z}}_c - Q_1\tilde{z}_c - Q_2\Xi_c - \Gamma\right) \tag{34}$$

where matrices Q_1 and Q_2 are given in (5),(28).

Since $\tilde{z}_c \to z_c$, then $\tilde{e}_z \to e_z$, and thus

$$\dot{\tilde{z}}_c - Q_1\tilde{z}_c - Q_2\Xi_c - \Gamma \to 0 \tag{35}$$

The sliding mode dynamics (34) asymptotically approach the homogeneous matrix differential equations

$$\dot{e}_z = (Q_1 - KQ_2)e_z, \quad e_\xi = -Ke_z \tag{36}$$

The matrix K is selected to provide the desired eigenvalues in (36). Using the sliding mode existence condition $\sigma_i\dot{\sigma}_i < 0$ [2,3], the sliding domain can be identified on the switching surface $\sigma = 0$.

The stable system center for the multiple modular boost converters is parameterized in (29)-(31). The corresponding sliding mode controller is defined by (32), (33). The gain matrix K is selected to provide desired tracking error dynamics of the boost converter in the sliding mode (36) that occurs when $\tilde{z}_c \to z_c$ and $\tilde{e}_z \to e_z$ as time increases.

Remark. The achieved results are local since the model (4) is valid near the linearization point.

VI. Numerical Example and Simulation of Multiple Modular Boost Converters

The following circuit parameters are selected for the boost converter and sliding mode controller: $c_0 = 1, c_1 = 3, c_2 = 3, \omega_n = 2,\ R_{L_1} = R_{L_2} = 50\Omega$, $R_S = 0.5\Omega$, $L = 10mH,\ C = 5\mu F$, $V_{C_1} = 40V, V_{C_2} = 50V\ \ E = 20V$.

The circuit parameters give $\alpha = 0.0112$, $\gamma_1 = \gamma_2 = 0.894$, and operating points at $\xi_{10} = 4$, $z_{10} = 20.38$ and $\xi_{20} = 6.25,\ z_{20} = 46.23$. We identify the stable system center as (37):

$$\tilde{z}_c^{(3)} + 3\tilde{z}_c^{(2)} + 3\tilde{z}_c^{(1)} + \tilde{z}_c = -\left(P_2\theta_c^{(2)} + P_1\theta_c^{(1)} + P_0\theta_c\right) \tag{37}$$

Substituting the parameters into Eqs. (5), (28), and (31) yields the numerical results for the P and Q matrices.

The command profile is formed as Ξ_c in (28). Once the transient in the stable system center (30), (31) is complete and $\tilde{z}_c \to z_c$, the sliding mode (31) becomes

$$\dot{e}_z = \left(\begin{bmatrix} 0.20727 & -0.00715 \\ -0.01747 & 0.128630 \end{bmatrix} - K\begin{bmatrix} -1.99527 & 0.00715 \\ 0.017468 & -1.91663 \end{bmatrix}\right)e_z .$$

Choosing $K = diag\left[\text{-}5.11587, \text{-}5.2847\right]$ yields the eigenvalues $\lambda = \left[-10, -10\right]$.

The parallel boost (multiple modular) converters, described by (1), (2) and the sliding mode control (32), (33) were simulated. The results are shown in Figs. 1 and 2. The plots are the reverse transformed variables and thus are the actual voltages and currents in real time. High accuracy output tracking is demonstrated in Fig. 1. The essentially unstable internal variables z_i are stabilized and follow the stable system center profile in (29), (30), (31) and in Fig. 2. Apparently, the control channels are decoupled, since any change in the command profile of one converter doesn't cause a transient in the other (parallel) converter output tracking.

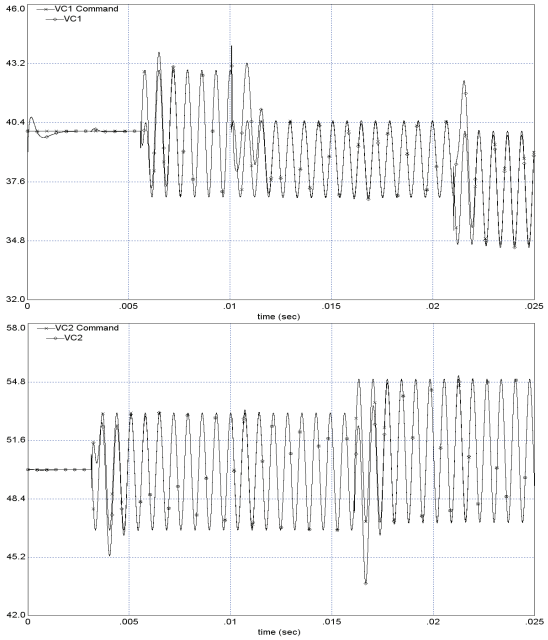

Figure 1: The Output Variable Tracking (Capacitor Voltages)

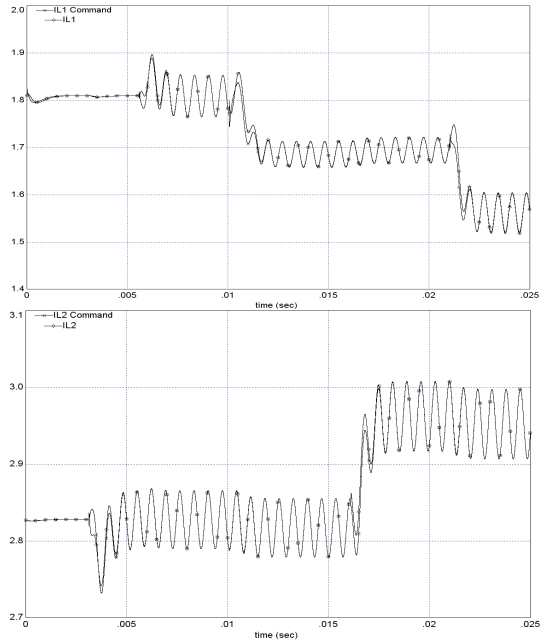

Figure 2 The Internal Variable Tracking (Inductor Currents)

VII. Conclusions

Direct tracking control of voltage is studied for multiple modular, and specifically, parallel, DC-to-DC boost power converters. Operating point analyses show that there are two possible operating points for each converter, and both result in nonminimum phase. It was shown analytically why one operating point is valid and the other is not. The sliding mode control design provides decoupling and high fidelity tracking of arbitrary voltage reference profiles given by an exogenous system in real time. A numerical example and simulation demonstrate the effectiveness of the sliding mode control design using the method of stable system center.

References

[1] Middlebrook, R. D., and Cuk S. Advances in Switched Mode Power Conversion, Pasadena, CA, Tesla, 1981.

[2] Utkin, V., Guldner, J., and Shi, J. Sliding Modes in Electromechanical Systems, Taylor and Francis, London, 1999.

[3] Edwards, C., and Spurgeon, S. Sliding Mode Control, Taylor & Francis, Bristol, PA, 1998.

[4] Sira-Ramirez, H., and Rios-Bolivar, M. Sliding Mode Control of DC-to-DC Power Converters via Extended Linearization. IEEE Transactions on Circuits and Systems - Fundamental Theory and Applications, 1994; 41(10), pp 652-661.

[5] Shtessel, Y. B., Raznopolov, O. A., and Ozerov, L. A. Control of Multiple Modular DC-to-DC Power Converters in Conventional and Dynamic Sliding Surfaces. IEEE Transactions on Circuits and Systems, Part I, 1998; 45(10), pp. 1091-1101.

[6] Zinober, A., Fossas, E., Scarratt, J., and Biel, D. Two Sliding Mode Approaches to the Control of a Buck-Boost Converter. Proceedings VSLT-9 1998; Orlando, FL, pp. 118-123.

[7] Fossas, E., and Zinober, A. Adaptive Tracking Control of Nonlinear Power Converters. Proceedings of ALCOSP 2001; Como, Italy, pp. 261-266.

[8] Sira-Ramirez, H. Flatness and Trajectory Tracking in Sliding Mode Based Regulation of DC-to-AC Conversion Schemes. Proceedings of the Conference on Decision and Control, 1999; Phoenix, AZ, pp. 4268-4273.

[9] Fossas, E., and Olm, J. M., Asymptotic Tracking in DC-to-DC Nonlinear Power Converters. Discrete and Continuous Dynamical Systems, Series B, Vol. 2, No. 2, May 2002, pp. 295-307.

[10] Sira-Ramirez, H., On the generalized PI sliding mode control of DC-to-DC power converters: a tutorial. International Journal of Control, No. 9/10, 2003, pp. 1018-1033.

[11] Shtessel, Y., Zinober, A., and Shkolnikov, I., "Sliding Mode Control of Boost and Buck-Boost Power Converters Using Method of Stable System Centre," Automatica, 2003, Vol. 39, Issue 6, June 2003, pp. 1061-1067.

[12] Shtessel, Y., Zinober, A., and Shkolnikov, I., "Boost and Buck-boost Power Converters Control via Sliding Modes using Method of Stable System Centre," Proceedings of the Conference on Decision and Control, pp. 340-345, December 2002.

[13] Isidori, A. Nonlinear Control Systems, Springer-Verlag. London, 3rd edition, 1995.

[14] Shkolnikov, I., and Shtessel, Y. "Tracking a Class of Nonminimum Phase Systems with Nonlinear Internal Dynamics via Sliding Mode Control using Method of System Center," Automatica, Vol. 38, Issue 5, May 2002, pp. 837-842.

[15] Levant, A. Robust exact differentiation via sliding mode technique, Automatica, 34(3), 1998, pp. 379-384.

[16] Fliess M., Sira-Ramírez, H., and Márquez, R. Requlation of nonminimum-phase outputs: A flatness based approach. In Perspectives in Control, D. Normand-Cyrot (Ed.), Springer-Verlag, 1998.